Lumbar Spine Injury Biomechanics

16

Brian D. Stemper, Frank A. Pintar,
and Jamie L. Baisden

Abstract

The primary biomechanical function of the lumbar spine is to bear the weight of the torso, head-neck, and upper extremities and support physiologic movement. The lumbar spinal column resides vertically between the thoracic spine and sacrum, and consists of five bony vertebrae interconnected by soft tissues including the intervertebral discs, ligaments, and muscles to maintain the integrity of the column under physiologic and traumatic environments. Injuries secondary to excessive deformations or loading resulting from external dynamic forces such as falls, or in military environments, aviator ejections, helicopter crashes or underbody blasts, can result in fracture of the lumbar spine with or without mechanical and clinical instability, and loss of normal function. These types of injuries can have significant consequences for the patient. Mechanically-induced traumas are transmitted to the lumbar spine in a variety of different ways. For example, axial or eccentric compressive forces transmitted to the lumbar spine through a vehicle seat sustaining high-rate vertical acceleration may result in different fracture types (e.g., burst fracture versus anteriorly-oriented wedge fracture), lead to mechanical instability, and impair normal daily activities. These acute consequences are in addition to the chronic effects of lumbar spine trauma including chronic back and lower extremity pain due to spinal degeneration, spinal cord or nerve root injury, or loss of lower limb sensation and function. This chapter outlines lumbar spine injury classification including mechanisms and clinical implication, describes experimental techniques used to understand injury mechanics,

B.D. Stemper, Ph.D. (✉) • F.A. Pintar, Ph.D.
Neuroscience Research Lab, Department of Neurosurgery, Medical College of Wisconsin, Milwaukee, WI, USA
e-mail: bstemper@mcw.edu; fpintar@mcw.edu

J.L. Baisden, M.D.
Department of Neurosurgery, Medical College of Wisconsin, Milwaukee, WI, USA
e-mail: jbaisden@mcw.edu

N. Yoganandan et al. (eds.), *Accidental Injury: Biomechanics and Prevention*,
DOI 10.1007/978-1-4939-1732-7_16,

and provides a listing of biomechanical fracture tolerance and injury criteria from experimental studies incorporating human cadavers. Due to the breadth of literature on lumbar spine injury mechanics, this chapter is not intended to be comprehensive. Rather, the reader will be provided with a overview of concepts relevant to the contemporary understanding of lumbar spine injury mechanics and tolerance.

16.1 Biomechanically Relevant Anatomy

The human spinal column has a sigmoid shape when viewed laterally, or in the sagittal plane. It is composed of 33 vertebrae interconnected by fibro-cartilaginous intervertebral discs in the anterior aspect, articular facet joints postero-laterally, and ligaments spanning adjacent vertebrae in multiple locations across the segment. Typically, there are seven cervical, twelve thoracic, five lumbar (L1–L5, Fig. 16.1), five fused sacral, and four separate vertebrae combined to form the coccyx. Among these, only the cervical, thoracic, and lumbar are flexible. In the sagittal plane, cervical and lumbar regions have an anteriorly convex shape, and the thoracic spine and sacrum are anteriorly concave. The lumbar spine is located in the abdominal body region and is the focus of this chapter.

16.1.1 Vertebrae

The five lumbar vertebrae are aligned with a prominent convex curvature in the lateral or mid-sagittal plane, otherwise known as lordosis. Lumbar vertebrae consist of an outer casing of dense and compact cortical bone. The interior part of the body is composed of cancellous bone aligned in lattice manner to resist axial force while minimizing mass, the effectiveness of which is proportional to its density. Lumbar vertebrae consist of the large body ventrally and posterior elements dorsally (Fig. 16.1). Extending from the vertebral body and moving posteriorly are the pedicles, transverse processes, articular processes forming the facet joints, laminae, and spinous processes. The vertebral foramen is a prominent feature of the lumbar vertebrae and is formed by the posterior aspect of the vertebral body and medial aspects of the pedicles, articular processes, and laminae. Extended from the base of the cranium and formed by all 33 vertebral foramina is the spinal canal, through which the spinal cord traverses. The cord transforms into the cauda equina near the second lumbar vertebra. Nerve roots exit the spinal canal at every vertebral level through the intervertebral foramina, formed by the postero-lateral aspect of the vertebral body, cranial and caudal aspects of opposing pedicles, and the anterior aspect of the articular processes.

The vertebral bodies form the most massive portion of the vertebra, are located anteriorly, and

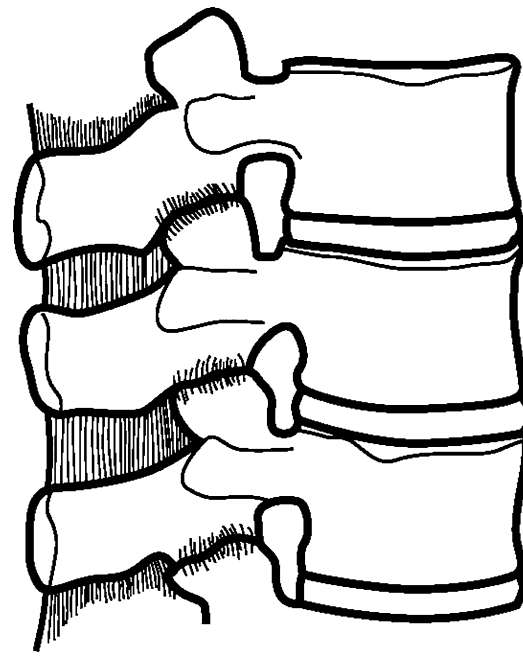

Fig. 16.1 Normal lumbar spine

are largest in the lumbar region, compared to thoracic and cervical regions. Lumbar vertebral bodies have relatively flat and kidney-shaped cranial and caudal surfaces. Transverse processes extend laterally from the pedicles. Facet joints form between opposing surfaces of the articular processes with joint surfaces oriented ventral-laterlly for the cranial processes and dorso-medially for the caudal processes. The pars interarticularis lies between superior and inferior facet joint processes. The large, flat, and vertically oriented spinous processes are located at the dorsal aspect of the vertebrae, are largest in the cranial region and decrease in size at the caudal levels. The five bony vertebrae of the lumbar spine are interconnected by soft tissues and joints, as described below.

16.1.2 Endplates

The endplates are the cranial and caudal surfaces of the vertebral bodies and form a thin cartilaginous interface between the bony vertebral body and the fibrocartilaginous intervertebral disc. The endplates are composed of hyaline cartilage. They are fused to the vertebral body by a calcium layer through which small pores penetrate for the nutrition of the intervertebral disc. The inferior zone of the vertebra remains in contact with the cartilage by the lamina cribrosa, the sieve-like surface. Osmotic diffusion occurs through this layer.

16.1.3 Intervertebral Discs

Intervertebral joints consist of a form of cartilaginous joint known as a symphysis. The primary component of the symphysis is the intervertebral disc, although the endplate (discussed above) is also a component. Lumbar intervertebral discs are located between adjacent vertebral bodies from the thoracolumbar junction (T12–L1) through the lumbo-sacral junction (L5–S1) and are connected to the bodies by the endplates. Their concentrically arranged components are: the outer alternating layer of collagen fibers forming the peripheral rim of the annulus fibrosus; a fibrocartilage component forming a major portion of the annulus fibrosus; the transitional region between the central nucleus pulposus (core), where the annulus fibrosus and the nucleus pulposus merge; and the nucleus pulposus made of a soft, pulpy, highly elastic mucoprotein gel containing various mucopolysaccharides, collagen matrix and water with relatively low collagen fibril. Intervertebral discs attach to the vertebral bodies centrally via the endplates and peripherally via the annulus fibers and ligaments. While some of the annulus fibers blend into the anterior and posterior longitudinal ligaments, others attach to the rim of the vertebra. The disc resists axial compression and tension, lateral and anteroposterior shear, and axial rotation. The shape of the disc in the lumbar spine is such that the lordotic curvature is maintained by the greater height ventrally than dorsally.

16.1.4 Ligaments

Ligaments are multilayered and composed primarily of elastin and collagen in different rations. In very general terms, collagen adds strength to the ligament whereas elastin adds elasticity. Spinal ligaments connect adjacent vertebrae (e.g., interspinous ligament) or extend over several segments (e.g., anterior longitudinal ligament). They are uniaxial structures. As such, they are capable of resisting only tension and buckle under compression. The anterior longitudinal ligament (ALL) runs from the occiput to the sacrum. It consists primarily of long, arranged collagen fibers which are aligned in interdigitizing layers. The deep layer extends only to adjacent vertebrae, the middle layer over a few vertebral levels, and the outer over four to five levels. This stratification is of significance in regulating physiologic motion. This ligament functions to prevent hyperextension and excessive distraction; it is functionally active in extension and rotation. The posterior longitudinal ligament (PLL) originates from C2, continues to the coccyx, and is located on the dorsal surface of the vertebral bodies. While this multilayered ligament closely adheres to the disc annulus, attachments to the vertebral bodies are minimal. It is broader in the area of the intervertebral disc and

very thin in the area of the vertebral bodies. Deeper layers span only the intervertebral disc and superficial layers can extent across multiple vertebral segments. The cross-section is considerably smaller and the tensile response is weaker than ALL. The ligamentum flava span between adjacent surfaces of laminae and are discontinuous, spanning from the cranial surface of the caudal vertebra to the caudal surface of the cranial vertebra. Ligamentum flava are present from C2–C3 to the sacrum. These ligaments are also termed yellow ligaments due to their appearance. Laterally, it is confluent with the joint capsules. Eighty percent elastin, and under some tension preload at rest, ligamentum flava are quite effective in returning the laminae to their resting positions following flexion. Capsular ligaments are intimate to the facet joint capsule and attach to the vertebrae adjacent to the articular joint. Their fibers are aligned normal to the facets, limiting distraction and sliding of the facet joints and hyperflexion of the segment. The interspinous ligaments connect adjacent spinous processes and are met by the ligamentum flavum anteriorly and the supraspinous ligament posteriorly. The supraspinous ligament is a fibrous ligament running along the distal extent of the spinous processes from seventh cervical vertebra to the sacrum. Interspinous and supraspinous ligaments act to resist flexion bending.

16.1.5 Facet Joints

Facet joints are articular joints that are located postero-laterally to the intervertebral disc at each vertebral segment (T12–L1 through L5–S1). There are two facet joints per segment (right and left sides). The joints are formed by the superior articular process from the caudal vertebra (facing dorso-medially) and the inferior articular process from the cranial vertebra (facing ventro-laterally). Opposing surfaces of the articular processes consist of a smooth and resilient layer of hyaline or articular cartilage. Surrounding the joint is a joint capsule and capsular ligament. Capsular ligaments are composed primarily of collagenous fibers and provide resistance to joint distraction that can occur during a variety of segmental movements. The joint capsule, also known as the synovial membrane or articular capsule, forms a complete envelope around the joint and acts to maintain joint integrity by containing the synovial fluid. The synovial fluid facilitates articulations and allows for 'gliding' of opposing articular surfaces that occurs during physiologic motions including flexion/extension, lateral bending, and axial rotations.

16.2 Injuries to the Spine

Injuries to the lumbar spine result from direct violence to the column or specific vertebrae. Unlike penetrating trauma, violence to the spine can most commonly be attributed to gross motions or acceleration of the body/torso. Examples include anterior bending of the torso resulting in flexion loads on the lumbar spine or vertical acceleration of the pelvis leading to axial compressive loads on the lumbar column. Loads placed on the tissues lead to deformation, with the magnitude, rate, and direction/type of loading responsible for the tissue distortion profile. Injury occurs when deformation exceeds physiologic limits of the tissue. The type and location of tissue deformation is dependent upon the applied load. Pure loads can take the form of linear forces or rotational bending moments. Linear forces can be applied in any direction, but are generally broken down into components based on axial tension/compression perpendicular to the horizontal plane, anterior-posterior shear perpendicular to the frontal plane, or lateral shear perpendicular to the sagittal plane. Likewise, bending moment components include flexion/extension in the sagittal plane, lateral flexion in the coronal plane, and axial twist in the horizontal plane.

16.2.1 Injury Classification

Lumbar spine injuries can be classified according to loading mechanism. Injuries can occur under tension, compression, shear, or bending, although some of these mechanisms are less common due to the inherent characteristics of the in situ

lumbar spine. Compression-related injuries are most common type in the thoraco-lumbar spine [1, 2]. Compression injuries occur in any number of high-rate axial loading scenarios including parachuting, falls from height, and motor vehicle crashes [3–8]. These injuries also occur in a variety of military- and sporting-related activities including skiing, snowboarding, and other sporting accidents [9–12], aviator ejection [13–20], helicopter crash [21–23], and underbody blast [24–31]. Injury mechanisms involve the primary component of axial force that can be coupled with varying magnitudes of bending. Injury type and severity are controlled by the biomechanical aspects of the insult. Specifically, axial force applied through the center of rotation of an intervertebral segment results in burst fracture. Axial forces offset from the center of rotation of a segment develop coupled bending moments, with greater offset distances resulting in greater moment magnitudes. Axial forces offset anteriorly, posteriorly, or laterally result in flexion-related injuries, extension-related injuries, or lateral bending-related fractures, respectively.

Tension and shear injuries can also occur in the lumbar spine. Tension (distraction) of the lumbar column is not a common loading scenario for humans. However, localized distraction occurs in different tissues during bending. For example, during forward flexion the anterior structures of the lumbar spine sustain localized compression loading. However, tissues posterior to the axis of rotation are distracted. This is particularly relevant for soft tissues such as ligaments and facet joint components, although bony fractures can also result from localized distraction (see Chance Fracture below). Likewise, shear injuries can affect he lumbar spine in some cases. However, the coupled effect of abdominal tissues most often transforms shear loading applied to the abdomen into bending of the spine. This section outlines different types of lumbar spine fractures, highlighting biomechanical mechanisms and briefly indicating the acute clinical outcome.

Burst fractures result from pure compression transmitted directly along the line of the vertebral bodies (Fig. 16.2). Due to the inherent lordotic curvature of the lumbar spine, pre-flexion is necessary to induce a purely compressive state [32]. From a biomechanical perspective, a relatively uniform compressive load is applied across the axial plane of the vertebral body. This results in loss of vertebral body height due to fracture of anterior and posterior cortices. Axial force also leads to fracture of one or both endplates, forcing the intervertebral disc nucleus into the vertebral body, and resulting in a burst pattern [32, 33]. High energy fractures can result in retropulsion of bony fragments into the spinal canal and associated neurological deficit. Posterior element fractures may also be involved, but are not required for this classification. Ligaments commonly remain intact and the spine is mechanically stable. These injuries have been considered to be clinically stable or unstable. Ferguson and Allen reported that these fractures were generally stable, but other clinicians have reported progressive neurological injury or advancing post-injury deformity [33–35].

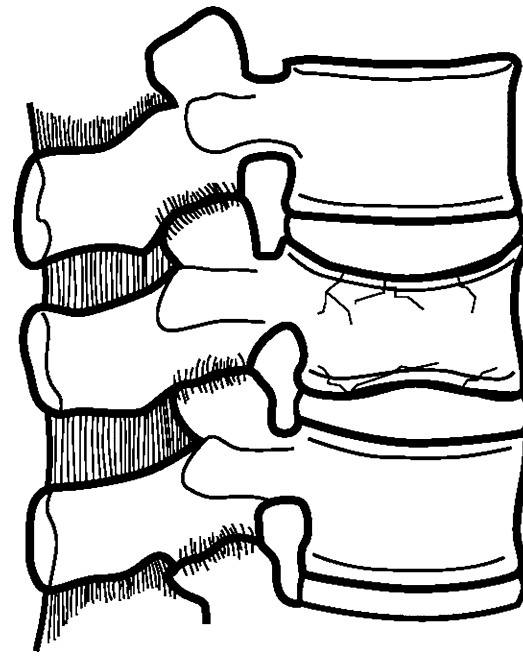

Fig. 16.2 Burst fracture

Anterior wedge fractures result from axial compression combined with flexion [36] or flexion alone [32] (Fig. 16.3). This combination can result from axial loads applied anterior to the

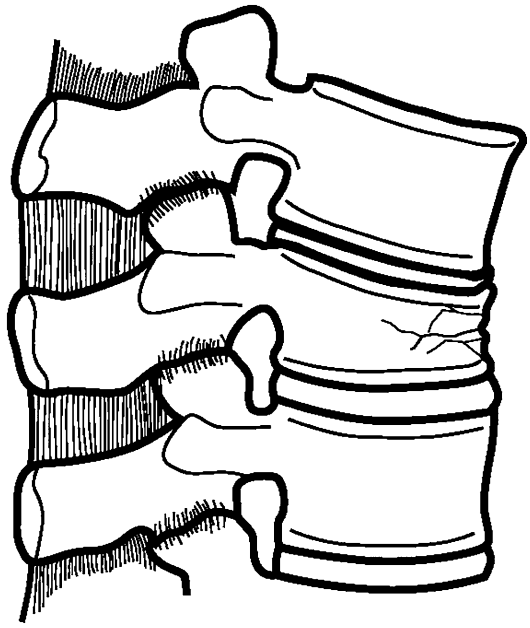

Fig. 16.3 Anterior wedge fracture

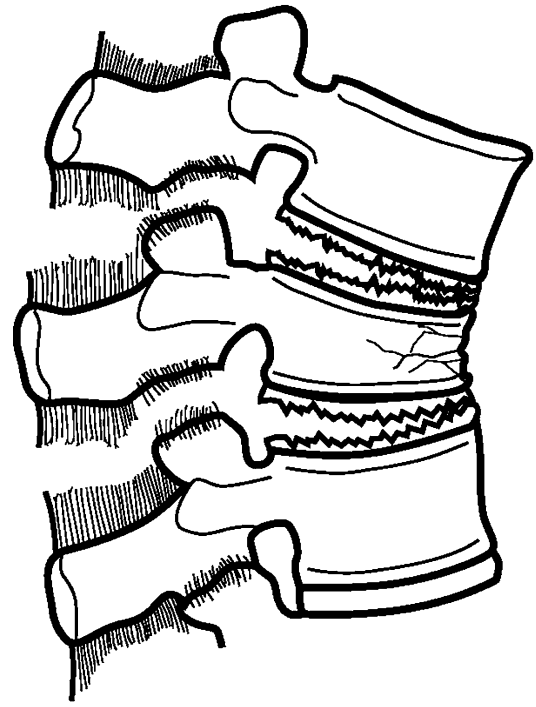

Fig. 16.4 Fracture dislocation including body fracture and facet dislocation

center of rotation of the vertebral segment or axial loading combined with anterior bending of the torso. In terms of biomechanics, tissues anterior to the center of rotation (e.g., anterior aspect of the vertebral body) sustain compression whereas middle- and posterior-column tissues (e.g., dorsal to the sagittal plane center of the vertebral body) are subjected to tension. Fractures affect the vertebral body and involve greater loss of body height anteriorly than posteriorly. In many cases, the posterior body height is unaffected. This results in a wedge-shaped profile as seen on lateral X-rays. While dynamic compressions are likely greater, wedge fractures typically present with less than 50 % anterior body height loss due to post-injury restitution. Slight and moderate wedge fractures are stable as the posterior aspect of the vertebral body and posterior ligamentous complex remain primarily intact [37]. Severe wedge fractures can occur with or without disc injury and involve disruption of the posterior ligamentous complex including ligamentous rupture or spinous process fracture. These fractures are unstable and typically referred to as fracture dislocations, which will be discussed below.

Wedge fractures can also occur laterally. Two mechanisms have been proposed to result in lateral wedge fractures. Flexion combined with rotation is the more commonly cited mechanism [2, 36], although Ferguson implicated compression combined with lateral bending [33]. Both mechanisms result in unilateral wedging, with the opposite side remaining intact, attributed to compression on the concave side and tension on the convex side. Radiographically, these injuries are evident in a frontal plane wedge-shaped profile when viewed on anterior-posterior X-rays. The lumbar column may also appear to have a lateral curvature centered about the injured level. Nicoll describes a unilateral wedging combined with transverse process fracture on the convex side and posterior intervertebral joint fracture on the concave side [2]. These injuries are generally considered to be clinically unstable, often associated with prolonged unilateral neurological deficit.

Fracture dislocation is a generic terms that refers to a condition involving fracture of the vertebra coupled with dislocation [36] (Fig. 16.4).

Dislocations can also occur in the absence of any bony fracture. These injuries commonly include rupture of the posterior interspinous ligament [2]. Depending on the status of the capsular ligaments, facet dislocation can occur, resulting in conditions involving upward subluxation, perching, forward dislocation, or forward dislocation with locking [2]. Kaufer and Hayes classified fracture dislocations into five groups based on the presence and type of anterior and posterior fracture or dislocation [38]. The mechanism for these injuries often involves flexion coupled with axial rotation or lateral bending. The coupled bending component is necessary in the lumbar spine region due to the inherent stability of the column, which can be attributed to the large vertebral bodies, wide and flat intervertebral discs, and well developed longitudinal ligaments. In the case of axial rotation, one or both articular processes can fracture causing the upper vertebra to rotate about the lower, breaking off a wedge-shaped section from the anterior region of the inferior vertebral body. A large coupled shear component can also contribute to fracture dislocations [36]. Fracture dislocations are clinically unstable with a propensity toward progressive deformity and acute neurological deterioration [2, 33, 38].

Chance fractures were first described by G.Q. Chance in 1948 [39] (Fig. 16.5). The mechanism of injury involves flexion coupled with distraction. Fractures initiate in the posterior aspect of the neural arch, often including the spinous process, and extend anteriorly into the posterior aspect of the vertebral body, terminating in an upward curve that extends toward the superior endplate just anterior to the neural foramen. These fractures occur in the absence of anterior vertebral body disruption or dislocation of the facet joints. The mechanism of these injuries is attributed to hyperflexion plus distraction. In many cases, these injuries were thought to result from the use of a lap seatbelt in automobile collisions [40, 41]. This mechanism is particularly relevant for improperly positioned lapbelts or pediatric occupants with immature pelvis to support the restraint [40–42], although other authors claim these injuries are rare in children 43. In these cases, the lapbelt would function as a fulcrum for the spine to rotate about, resulting in tension injuries of the posterior lumbar vertebra. Incorporation of a properly worn shoulder belt to support the torso has minimized the likelihood of these injuries. From a clinical perspective, these injuries are considered to be stable, with little chance of neurological deficit [2, 42].

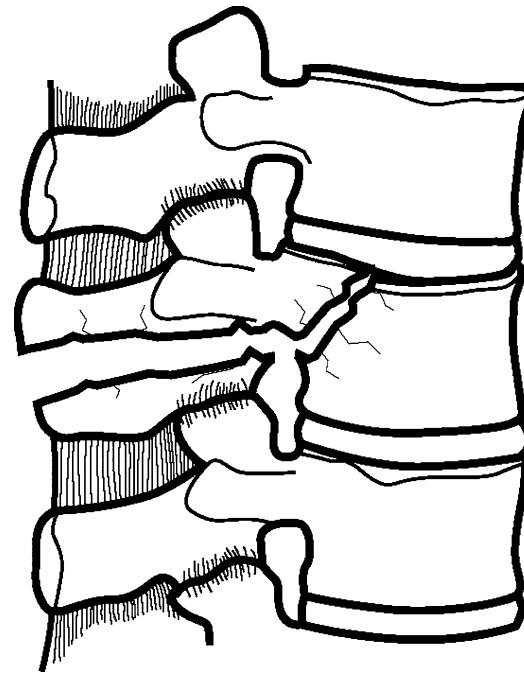

Fig. 16.5 Chance fracture

16.3 Loading Issues

Numerous biomechanical investigations of the lumbar spine have been conducted using whole body cadaveric specimens, lumbar columns, spine segments, and isolated tissues. These investigations have quantified quasi-static and dynamic physiologic, degenerated, and traumatic responses of the lumbar spine under a variety of loading conditions including compression, bending, and shear. A comprehensive review of lumbar spine biomechanical research is beyond the scope of this chapter. Rather, this chapter aims to highlight experimental biomechanical methods and provide tolerance-related information for the lumbar spine. Due to the prominence of axial loading

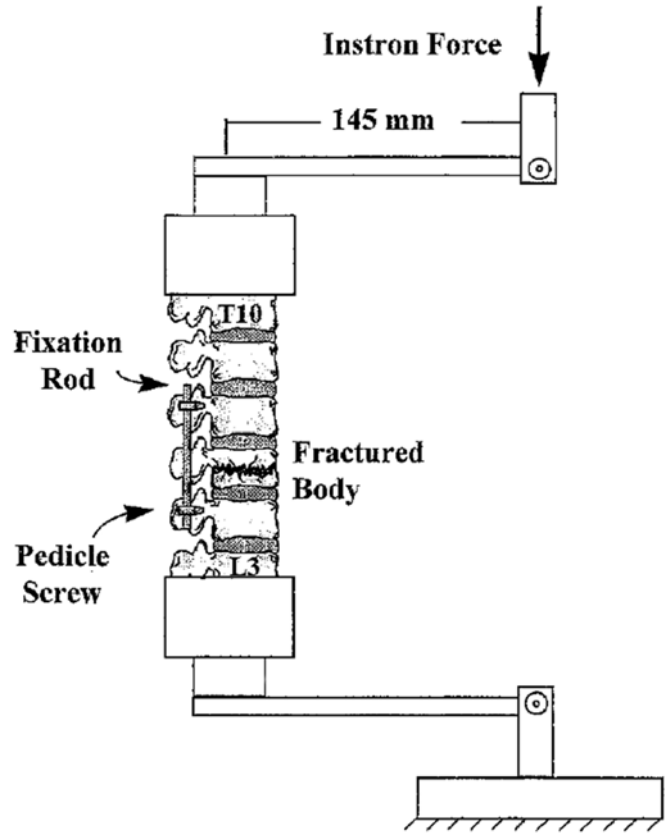

Fig. 16.6 Experimental model incorporating an electro-hydraulic testing device to induce compression-flexion on a lumbar spine column (From Mermelstein et al., Spine 1998 with permission)

on lumbar spine injury mechanics, a significant portion of existing research has focused on this mode. Accordingly, this chapter will focus primarily on experimental studies of axial loading. The following sections provide a description of three experimental protocols that have been used to investigate dynamic axial tolerance of lumbar spine components, and a fourth method incorporating whole body specimens.

16.3.1 Electro-hydraulic Testing Device

A considerable amount of experimental effort has been applied toward the understanding of lumbar spine injury tolerance during dynamic axial loading. Much of that research has been conducted using either electro-hydraulic testing devices or weight-drop apparatuses. Research incorporating electro-hydraulic testing devices have been conducted using whole lumbar columns [44–46], column segments (e.g., two-vertebra motion segments) [47–49], isolated vertebral bodies [50–58], and components including ligaments and annular tissues [59–75]. These devices apply quasi-static or dynamic axial loads using the piston of the electro-hydraulic device. An advantage of electro-hydraulic testing devices is that piston excursion is computer controlled, which leads to a high level of control over the loading versus time pulse, although these devices are somewhat limited in loading rate. Loads can be distributed across the vertebral endplate, applied at a distance from the specimen to induce a bending moment, or locally applied to a specific region of the endplate or intervertebral disc using an indentor. By design, electrohydraulic testing devices are typically uniaxial and compression is the most common loading mode. However, the devices can also impart compression combined with bending through application of axial load at a distance from the center of segmental or column rotation using a moment arm or vertebral arch (Fig. 16.6). For example, compression-flexion loading can be induced through load

application to a moment arm extending anteriorly from the cranial vertebra. Likewise, compression-extension and compression-lateral bending are induced using moment arms extending posteriorly or laterally. Oblique loading can be produced through application of the load in the anterior- or posterior-lateral locations. Distance of the load application from the center of rotation controls the ratio of axial load to bending. Load application at a greater distance from the center of rotation results in a higher ratio of bending to axial load. Likewise, load application closer to the center of the vertebra leads to a higher component of compression.

Testing is generally conducted with specimens in neutral position, although some series have applied flexion or extension loads to bias the initial position and study orientation effects [48]. Custom devices have the ability to apply axial tensile or compressive forces at loading rates up to 9 m/s. However, testing of lumbar columns and segments has generally been conducted at quasi-static rates as low as 1.0 mm/min [47] or dynamic rates up to 1.0 m/s [46]. Testing of individual vertebrae has been conducted at rates up to 2.5 m/s [51]. Specimens can be instrumented, with reflective markers, accelerometers, and strain gauges to obtain level-by-level kinematic (displacement and angulation) or localized compressive information. Loads at the impacted and distal ends are recorded using load cells and localized (level-specific) loads can be computed by coupling load cell data with kinematics information. Because of the controlled nature of load application using the piston, dynamic subfailure loading can be used to quantify the physiologic response of lumbar tissues. Likewise, injuries produced during dynamic loading can be correlated with biomechanical measures to derive injury tolerance information. However, it is difficult to achieve a constant velocity during biofidelity testing as the piston has to initiate its travel from rest, and deceleration initiates prior to the point of peak displacement. Constant loading rates can be obtained with piston overshoot, by setting piston displacement to a maximum level well beyond the expected fracture displacement. Inertial effects of the piston require compensation for force measurements from load cells attached to the piston and in-line with the loading vector.

Electro-hydraulic testing devices are also useful for testing of isolated tissues under appropriate loading modes. Although tension of the lumbar spine is rare, specific soft tissues sustain tension during different loading situations. For example, dorsal soft tissues sustain tension during segmental flexion. Likewise, due to Poisson's effect, intervertebral disc annular tissues sustain tension during segmental compression. Similar to compression, tension loading rates can vary from quasi-static to dynamic and maximum distraction can be maintained within the physiologic range or can enter the traumatic realm. A variety of biomechanical studies have been conducted using electro-hydraulic testing devices to quantify tensile response of lumbar spine ligaments [63–65, 67, 68, 70, 72] and intervertebral disc material [60, 61, 66, 76].

16.3.2 Weight-Drop Apparatus

The weight-drop apparatus is another method of load application similar to the electro-hydraulic testing device, with the primary exception that loads are applied by dropping a weight onto the cranial end of the specimen instead of using the piston (Fig. 16.7). Numerous studies have been conducted using the weight-drop apparatus and incorporating 2- and 3-vertebrae segments [77–79] or longer lumbar columns [80–83]. This test setup applies dynamic compressive loads by impacting the spine using a decelerated weight. The weight is accelerated by gravity until impacting the spine and is either guided or allowed to fall without constraint. Similar to the electro-hydraulic testing device, compression is the most common loading mode, although compression combined with bending can be applied through application of axial load at a distance from the center of segmental or column rotation using a moment arm.

Testing is most commonly conducted with specimens in neutral position, although pre-flexion has been applied in some cases [81, 84, 85]. Rate of loading is controlled by mass of the impactor and its closing velocity (i.e., velocity at the time of

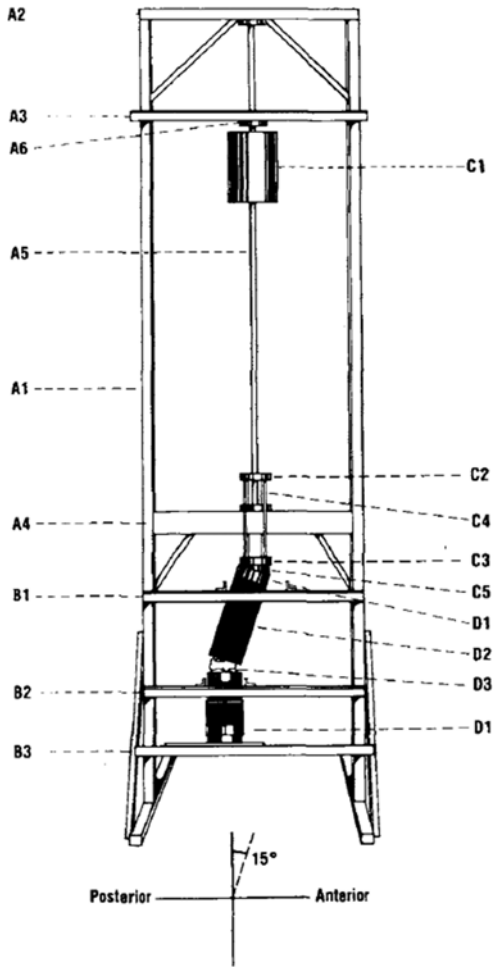

Fig. 16.7 Experimental model incorporating a weight-drop device to induce compression-flexion on a lumbar spine column (From Cotterill et al., J Orthop Res 1987 with permission)

impact). Control of maximum compression is difficult as this method relies on specimen impact to halt the excursion of the dropped weight. Loading rate can be quantified as the rate of load application (N/s). Specimens can be instrumented, with reflective markers, accelerometers, and strain gauges to obtain level-by-level kinematic (displacement and angulation) or localized compressive information. Loads at the impacted and distal ends are recorded using load cells and localized (level-specific) loads can be computed by coupling load cell data with kinematics information. Subfailure testing is performed by dropping the weight from a height that does not induce fracture and is used to quantify the physiologic response of lumbar tissues. Likewise, injuries produced during dynamic loading can be correlated with biomechanical information to derive tolerance information. However, it is difficult to achieve a constant velocity during biofidelity testing as deceleration of the dropped weight initiates immediately upon contact with the specimen.

16.3.3 Drop Tests

Drop tests are used to replicate vertical acceleration conditions in either component or whole body cadaver tests (Fig. 16.8). Benefits of this experimental setup realistic loading and boundary conditions and the ability to relate injury tolerance to external metrics associated with the loading environment (i.e., acceleration of the lumbar spine base). These tests involve a drop tower of varying height, at least one platform connected to a guide rail using linear bearings or a cart mechanism, and pulse-shaping material at the bottom of the tower to modulate characteristics of the deceleration pulse. Testing involves mounting the specimen to the platform, raising the platform to a specific height, release with gravity accelerating the platform downward, and impact to the pulse-shaping material at the base of the drop tower. Characteristics of the deceleration versus time pulse are controlled using initial height, mechanical properties of the pulse-shaping material, and amount of pulse shaping material. Peak accelerations as high as 65 G with rates of onset as high as 2,500 G/s have been achieved using this model [86]. In general, greater peak accelerations can be obtained with drops from greater initial height and steeper rates of onset (i.e., shorter pulses) are obtained with stiffer pulse-shaping material. In the case of isolated components, similar biomechanical information can be collected to that for the weight-drop and electro-hydraulic testing devices including forces at the top and base of the specimen, three-dimensional spinal kinematics (e.g., linear and angular motions and accelerations), localized strains, and fracture information from acoustic sensors.

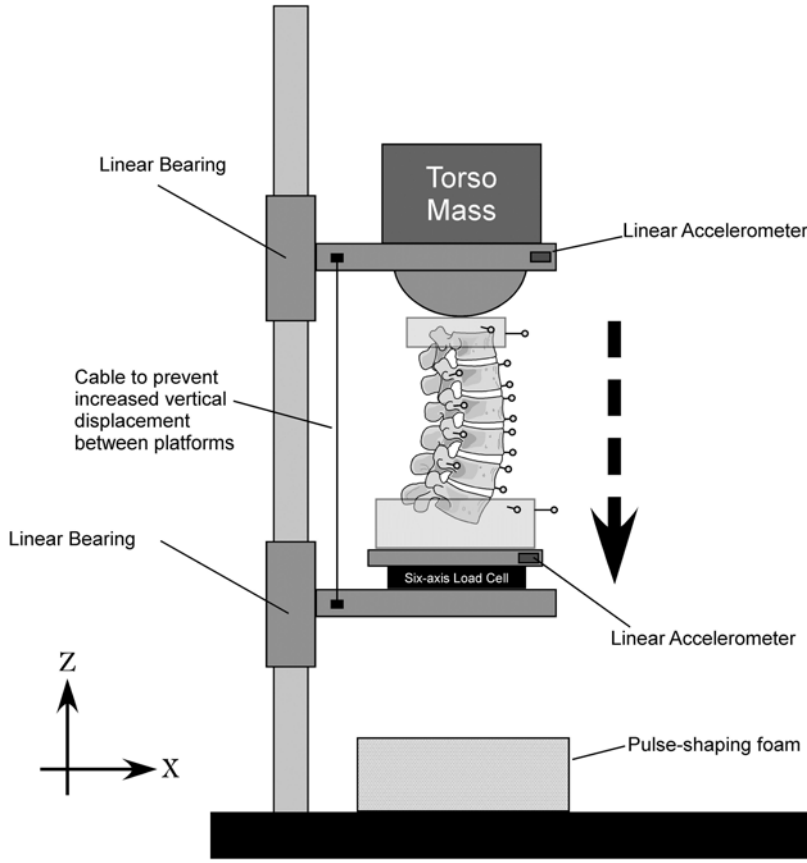

Fig. 16.8 Experimental model incorporating a drop tower apparatus to induce compression-flexion on a lumbar spine column (From Stemper et al., J Biomech Eng 2011 with permission)

A second decoupled platform with variable mass can be added to the cranial aspect of the spine to simulate the torso. The mass can be the same for all specimens tested under a given protocol, for consistency, or can be varied to mimic specimen-specific torso mass. Lumbar spine components can be tested in compression or, since the mass can be attached to the upper platform via a telescoping linkage and load application can be moved anterior-posteriorly, compression combined with flexion, extension, or lateral bending.

16.4 Specimen Details

Different types of experimental models exist to determine the biomechanical properties, replicate real-world injuries, derive injury mechanisms, and determine human tolerance in terms of variables such as forces and risk curves using the above described experimental techniques. Some of the more common experimental models are discussed in this section.

16.4.1 Isolated Components

Testing of isolated components such as vertebral bodies has been performed to quantify the structural or material response of the isolated vertebral body or endplate. Testing of vertebral bodies and endplates is typically performed using electro-hydraulic testing device with flat horizontal plate for bodies and an indentor for endplates [51, 87–90]. These tests have been conducted from quasi-static to dynamic rates. Axial force is measured

using a load cell, compression displacement is measured using two-dimensional videography or the piston LVDT, and vertebral body strain is measured using strain gauges. These types of testing are ideal for the quantification of high-rate material properties as loading conditions are controlled, repeatable, and applied directly to the tissue of interest.

Isolated soft tissues have also been tested to quantify the structural and material response. Those tests are typically conducted by distracting the specimen in tension using an electro-hydraulic testing device [61, 70]. Testing has quantified the quasi-static, dynamic, and viscoelastic response of isolated ligaments and annular tissues. Test specimens are commonly arranged in an I-shaped mechanical test specimen. However, attachment to the test frame can be difficult for smaller tissues (i.e., fascicles) and test coupons may be required [64].

16.4.2 Segmented Columns

Segmented column models are used to experimentally delineate the gross biomechanical responses of the spine at a macro level and determine tolerance characteristics. Effects of lordotic curvature are incorporated because more than one functional unit is used. Pre-alignment of the spine can be incorporated to account for effects of body posture. However, the degree of inclusion of these factors depends on the number of spinal segments. Consequently, these models tend to be more realistic from injury reproduction perspectives although failure responses of individual components cannot be quantified because the load-path at a segmental level is unknown. Three-dimensional motions of the intervertebral levels have been obtained at high rates of 1,000 samples per second. Two-dimensional motions using high resolution digital cameras can be obtained at much higher rates (~50,000 frames per second). Likewise, local accelerations and strains of individual vertebrae can obtained using accelerometers, strain gauges, and acoustic emission sensors to determine the timing of fracture or spinal instability. Positioning the segmented column on an x–y cross table mounted to the platform of an electro-hydraulic testing device is needed to achieve the intended posture or pre-alignment. The transmitted forces and moments can be recorded at the inferior end using a six-axis load cell. Forces and moments at the segmental level of injury may be estimated although the local dynamics are not known. High-speed video images can be taken to document macroscopic failures, high-speed x-rays can be obtained for bony fractures, and localized segmental motions analyses can be performed using this model. Strict control of the experimental loading conditions can be achieved using segmented columns. Testing can be conducted at injurious levels, or below the threshold for injury to quantify the physiologic response.

Another methodology to apply dynamic loads to the segmented column is using free-fall or drop techniques as described above. This involves fixing the ends of the column, applying preloads (if any), controlling alignment by techniques such as pre-flexing using cables, and dropping on to targets with known stiffness to modulate the pulse. Ensuing motions of the column following initial contact with the target may induce continuing loads and contribute to additional injuries. However, load limiters have been used to prevent this occurrence.

16.5 Biomechanical Data

A number of studies have been performed to characterize lumbar spine fractures and quantify biomechanical tolerance due to axial loading. Specific aims of these studies were to clarify the injury mechanism, observe fracture patterns, measure spinal canal occlusion, compare surgical instrumentation techniques, or understand biomechanics of injury. As mentioned above, in many cases, the electro-hydraulic testing device or weight drop models were employed. However, other studies have incorporated the alternative models described above. Physiologic and injury tolerance information has been derived from these studies. Although not comprehensive, some of the relevant findings are discussed below.

16.5.1 Compressive Load to Failure and Tolerance

Dynamic compression of isolated vertebral bodies using electro-hydraulic test devices has been used to define compressive tolerance of endplates or the body as a whole in the lumbar spine. Those studies have incorporated electro-hydraulic testing devices with indentor (endplate) or flat plate (vertebral body) attachments to the piston to load specimens under quasi-static or dynamic loads. Studies of endplate tolerance have demonstrated significant rate dependence [51] and regional dependence across the surface of the endplate [91]. Strength of the endplate was previously theorized to play a strong role in formation of vertebral burst fractures [32], one of the primary injury types sustained during high-rate dynamic axial loading. Endplate strength was previous correlated to bone mineral density of the vertebral body [92–94]. Because bone mineral density is known to decrease with age, eventually leading to osteoporosis, specimen selection for injury tolerance investigations is critical, and must be performed in light of the population of interest. This can minimize the necessity to scale injury tolerance values obtained from specimens with older ages or osteoporotic spines. Investigations of vertebral body fracture mechanics have generally demonstrated rate of loading effects on tolerance [50–52, 95]. For example, Ochia et al. subjected isolated lumbar vertebral bodies to compressive loading rates of 10 mm/s or 2.5 m/s and demonstrated significantly increased fracture tolerance at the higher loading rate [51]. Kazarian and Graves demonstrated a similar finding for the thoracic spine across loading rates of 0.09 mm/s, 9 mm/s, and 0.9 m/s [50]. A summary of vertebral body testing is provided in Table 16.1. For studies including severely osteoporotic spines, only data from normal and osteoporotic spines are included in the table.

Researchers investigating lumbar spine tolerance have long acknowledged the importance of loading rate as an influencing factor. This fact has particular relevance to the military environment, wherein injuries can occur across a variety of loading rates from relatively low rate (falls) to extremely high rate (underbody blast) [24, 27–30]. The weight-drop method (described above) was one of the first experimental models to impart high-rate axial loading to the lumbar spine, as first described by Hirsch and Nachemson in 1954 [96]. Perey later reported on injury types resulting from experimental modeling of axial compression using the weight-drop method [52]. These experiments produced approximate maximum loads between 10,300 and 13,200 N within 6.0 ms by dropping a mass of 15 kg from a height of 0.5 m. Endplate fractures occurred in 26 % of experiments; wedge-shaped vertebral compression fractures occurred in 8 %. Willen et al. produced more severe compression fractures (i.e., burst fractures) by dropping a 10 kg mass from 2.0 m onto 3-vertebrae thoracolumbar specimens [78]. That study qualitatively demonstrated an age dependence, wherein specimens from cadavers greater than 70 years of age tended to completely collapse in compression and vertebrae from cadavers less than 40 years of age sustained the comminuted fracture pattern characteristic of burst fractures as defined by Denis [97]. These experiments tend to agree with clinical literature that has reported burst fractures generally occurring in younger patients [98, 99]. Subsequent studies have provided confirming results to demonstrate that burst fractures are generally produced under high-rate loading scenarios [52, 78, 100–102]. Testing characteristics and fracture biomechanical data from these studies are summarized in Table 16.2.

Spinal orientation at the time of impact is a factor that has commonly been associated with influencing injury risk during axial loading the lumbar spine. Initial spinal orientation was shown

Table 16.1 Summary of vertebral body (VB) and endplate (EP) testing in literature

Parameter	Unit	Range
Investigated spinal levels	N/A	T12–L5
Testing velocity	m/s	0.01–4.0
VB fracture displacement	mm	2.3–6.5
VB fracture force	kN	4.9–14.9
VB fracture stress	N/mm^2	3.7–7.0
EP fracture force	N	55–170
EP fracture stress	N/mm^2	6.3–7.5

Table 16.2 Summary of short-segment weight-drop literature

Parameter	Unit	Range
Number of spinal levels	N/A	2–3
Impactor mass	kg	2.3–18
Initial impactor height	m	0.5–2.0
Impactor closing velocity	m/s	3.1–6.2
Spine angle	°	0–15
Fracture force	kN	5.3–13.2

to drastically affect the physiological level-by-level segmental kinematics of the lumbar column during dynamic axial loading applied using a drop tower apparatus [86]. Weight drop studies have incorporated protocols with lumbar spine specimens in neutral or pre-flexed positions. Panjabi et al. quantified the differences in fracture tolerance between 3-vertebrae spinal segments oriented in either neutral or 15° pre-flexed positions [102]. Pre-flexion decreased fracture tolerance by 7 % from 6.7 ± 2.0 kN in neutral position to 6.2 ± 2.3 kN for 15° of pre-flexion. Likewise, comparison between studies highlights decreasing tolerance for lumbar spines in pre-flexed positions. Testing of lumbar spines in neutral position resulted in fracture tolerance between 6.0 and 13.2 kN [52, 78, 102] Fracture tolerance was between 5.3 and 6.6 kN when spines were pre-flexed to 8° [100, 101]. Although the weight-drop model will not be incorporating in testing protocols for this project, effects of initial specimen orientation will be included in the test matrix to demonstrate differing injury tolerance between neutral position and orientations including flexion, extension, or lateral bending.

Fracture tolerance of lumbar segments and columns has been investigated using the electro-hydraulic testing apparatus setup in multiple investigations. Whole lumbar columns have demonstrated fracture tolerance of between 3,303 and 12,535 in one study [45] and 5,009 or 5,911 in another study [46]. However, both fractures were obtained at the cranial level in the second study, which may indicate failures resulting more from fixation artifact than axial loading conditions. Other studies using 3-vertebra segments have demonstrated effects of loading rate or specimen orientation. Langrana et al. investigated effects of

Table 16.3 Summary of short-segment electro-hydraulic testing device literature

Parameter	Unit	Range
Number of spinal levels	N/A	2–3
Testing velocity	m/s	0.01–2.5
Spine angle	°	−15–0
Fracture force	kN	2.8–12.4

Table 16.4 Summary of lumbar column electro-hydraulic testing device literature

Parameter	Unit	Range
Number of spinal levels	N/A	6–7
Testing velocity	m/s	1.0
Spine angle	°	0
Fracture force	kN	3.3–5.9

specimen orientation on fracture tolerance and demonstrated considerably lower tolerance for specimens tested in neutral position (2.8 ± 0.7 kN) than for specimens tested with 15° of pre-extension (5.8 ± 1.8 kN) [48]. Effects of specimen orientation are important for real-world application as occupants of different vehicles inherently have different seated postures which changes the orientation of the lumbar spine relative to the applied load and influences injury tolerance/risk. Another experimental study incorporating the electrohydraulic testing device model investigated effect of loading rate on fracture tolerance [103]. That study identified increasing fracture tolerance for higher rates of axial loading with specimens positioned in neutral posture. Fracture tolerance was 3.3 ± 1.2 kN for specimens tested at compression rates of 10 mm/s and 4.2 ± 1.7 kN for specimens tested at 2.5 m/s. Understanding rate effects on lumbar spine fracture tolerance has importance for the development of injury mitigation devices. For example, underbody blast is likely to load the lumbar spine at higher rates than aviator ejection, automotive, and fall environments. A summary of human cadaver experiments incorporating the electro-hydraulic testing device setup is provided in Tables 16.3 (short segment) and 16.4 (lumbar columns) below.

While short segment (2- or 3-vertebrae) experimental models provide controlled and repeatable testing protocols, application to the lumbar

column mechanics is somewhat limited due to limited incorporation of lordotic curvature and continuous ligamentous structures such as the anterior longitudinal ligament. In 3-vertebrae constructs, only on vertebra is exposed to traumatic loading, which changes the inherent biomechanics including level-by-level load transmission. Therefore, lumbar column testing may be more suited to the understanding of the physiological response and injury tolerance of the lumbar spine associated with axial loading environments.

Testing of whole column specimens was not reported until more recently. Yoganandan and colleagues tested full lumbar columns under quasi-static testing (2.5 mm/s) in the compression-flexion mode using the electro-hydraulic piston model [44]. Fracture occurred at an average load of 3.8 ± 0.5 kN. More recently, Duma et al. subjected whole lumbar columns to dynamic compression loading at a rate of 1.0 m/s [46]. Fracture tolerance in that study was reported as a combination of compression force and bending moment: 5.4 ± 0.5 N and 201 ± 51 Nm. Although the two studies are not directly comparable due to differences in experimental protocol including stress risers [44], it is worth noting that fracture tolerance increase by approximately 40 % under dynamic loading. This highlights a dependence of fracture tolerance on loading rate.

A limited number of investigations have focused on quantifying lumbar column tolerance using a drop tower apparatus [86]. Those studies focused on quantification of military loading rate effects on injury tolerance and location in lumbar columns. Aviator ejection and helicopter crash pulses were simulated with accelerations of 21 and 58 G, respectively. Rates of acceleration onset were 371 and 2,068 G/s. Fracture tolerance increased from 5.7 kN in the lower rate ejection tests to 6.7 kN in the higher rate helicopter crash tests, demonstrating a clear rate dependence. However, also important was that injury locations migrated from primarily upper lumbar spine (e.g., L1, L2) during ejection tests to lower lumbar spine (e.g., L3, L4) during higher rate helicopter crash tests. Unique kinematic data were also collected and used to inform isolated tissue studies.

Table 16.5 Summary of lumbar column drop tower literature

Parameter	Unit	Range
Number of spinal levels	N/A	6
Peak accelerations	G	20.7–65
Rates of onset	G/s	228–2,638
Vertebral body compression rate	m/s	0.5–1.25
Spine angle	°	0
Fracture force	kN	5.2–7.8

For example, two kinematic targets were placed on the anterior of each vertebral body to measure compression rates during fracture. During burst fractures sustained in ejection-simulating tests, vertebral bodies were compressed at rates below 1.0 m/s [95]. That compression rate increased up to 1.25 m/s during helicopter crash tests. A benefit of these studies is the ability to replicate seat, pelvis, or lower lumbar vertical accelerations in the controlled laboratory environment. A summary of these studies is provided in Table 16.5.

16.5.2 Tolerance Criteria

Injury metrics are used to predict occurrence or risk of injury under well-defined dynamic loading scenarios. Although it is more computationally expedient to represent injury tolerance using a single metric (e.g., axial force) and value (e.g., 6 kN), injury risk is often more precisely predicted using a complex computation. Injury metrics are often developed in conjunction with biomechanical testing of cadavers, wherein injuries can be produced under quantifiable and repeatable loading environments. Statistical analysis can then be used to quantify computational metrics that are most predictive of injury. Due to non-homogeneous geometry and material properties of the spine, injury metrics must be developed for specific loading environments and injury types. To date, there remains a gap in the development of a robust injury metric for the lumbar spine. For example, separate injury metrics have been developed in the cervical spine for automotive frontal and rear impacts.

Development of tolerance criteria for the lumbar spine initiated following medical reports of

thoraco-lumbar compression fractures sustained by military aviators during ejection from aircraft, which subjected the aviator to high-rate vertical accelerations [104–108]. Initial efforts focused on development of whole body tolerance [109, 110]. While providing useful performance envelopes and design targets for safety engineers, whole body metrics lacked specificity for injury mechanisms and types, such as thoracolumbar compression fractures. Focusing on the spine as a component, Latham developed a mechanical model consisting of lumped parameter elements that was mathematically represented by a second order differential equation accounting for deflection, damping, natural frequency and acceleration of the system [111]. Stech and Payne incorporated the model into an analysis of vertical accelerations, under the assumption that the spine was the primary load-bearing structure in that mode [112]. Their analysis included parameters determined using experimental research and computational analysis [113, 114]. That work was premised on the theory that deflection of the lumbar column, as predicted using their lumped parameter model, was the primary indicator of vertebral fracture. This work resulted in the determination of the Dynamic Response Index (DRI), which is a dimensionless parameter derived to represent the maximum spinal compression experienced during an acceleration event and predict the probability of spinal injury for different age groups [112]. For example, he 50 % probability of spinal injury was estimated to be a DRI value of 21.3 for occupants 27.9 years of age, which was the mean age of the U.S. Air Force aviator population in 1969. Accordingly, the Air Force set a maximum DRI safety level of 18 to represent a 5 % chance of spinal injury during ejection in specification MIL-S-9479B, the military standard for ejection seat systems in aircraft. Further investigations developed spinal injury probabilistic relationships with DRI based on operational data [115].

Where the DRI was developed under the theory that spinal injury is displacement controlled, other researchers have taken an alternate approach by investigating metrics correlating compressive force to injury. For example, Chandler reasoned that acceleration or DRI alone could not account for effects of occupant restraint loading [116]. Accordingly, he suggested that axial force measured between the lumbar spine and pelvis would more accurately account for injury risk. That study referenced work performed at the Federal Aviation Administration Civil Aeromedical Institute (CAMI) to develop a lumbar spine injury metric based on axial compressive force. Those studies measured axial load in the lumbar region of a human manikin subjected to vertical accelerations and demonstrated the influence of occupant positioning. Based on findings from that study, the General Aviation Safety Panel (GASP) recommended a load limit of 6,672 N for axial accelerations. This value corresponded to a DRI value of 19 and a spinal injury risk of approximately 9 %. The Federal Aviation Administration adopted that load limit as a pass/fail condition for their dynamic test procedure for seats within transport category aircraft.

As demonstrated in this brief review, DRI and axial compressive force are the primary lumbar spine injury metrics used to predict injury in vertical accelerative environments. However, these metrics do not fully account for non-uniformity in lumbar spine geometry/material properties and complex loading environments associated with off-axis or out-of-position situations. As demonstrated earlier in this review, these factors are critical in the prediction of injury risk and occurrence. For example, pure lumbar spine axial compressive force alone cannot cause anterior wedge fractures, and consequently lumbar spine injury susceptibility cannot be assessed using compressive forces and ignoring other biomechanical factors. As such, research efforts for the lumbar spine should investigate and develop lumbar spine injury metrics which are sufficiently robust and applicable regardless of the loading environment.

16.6 Summary

The purpose of the review has been to evaluate available biomechanical data relevant to lumbar spine injury tolerance. Research studies using

PHMS were reviewed with a focus on lumbar spine injuries and their mechanisms. Peak injury metrics and human injury risk functions developed from the forces, rotations, and moments measured were included.

The review discussed quasi-static and dynamic tests using lumbar columns, motion segments, and isolated tissues such as vertebral bodies. Dynamic loading protocols have incorporated electro-hydraulic test devices, weight drops, and drop towers. Testing velocity during isolated vertebral body and endplate testing was between 0.25 and 4.0 m/s. Weight drop studies have been conducted using short- and long-segment cadaveric models with mass between 2.3 and 18 kg impacting the spine at velocities between 3.1 and 6.2 m/s. Electro-hydraulic piston tests have been conducted using short- and long-segment models, as well as whole lumbar columns, at rates from quasi-static to 2.5 m/s. Drop tower studies have been conducted using whole lumbar columns at rates approximating military aviator ejection and helicopter crash. These tests have provided information regarding effects of lumbar spine posture at the time of impact on injury tolerance. Injury tolerance in these tests has been somewhat consistent, given the range of experimental conditions. Variation in fracture tolerance can likely be attributed to differing age/BMD of specimens incorporated in the studies, differing loading rates, and differing initial posture.

Acknowledgments The authors gratefully acknowledge the contributions Kim Chapman and the Zablocki VA Medical Center Medical Media for providing many of the figures used in this chapter.

References

1. Griffith HB, Gleave JR, Taylor RG (1966) Changing patterns of fracture in the dorsal and lumbar spine. Br Med J 1:891–894
2. Nicoll EA (1949) Fractures of the dorso-lumbar spine. J Bone Joint Surg Br 31B:376–394
3. Wang MC, Pintar F, Yoganandan N, Maiman DJ (2009) The continued burden of spine fractures after motor vehicle crashes. J Neurosurg Spine 10:86–92
4. Richards D, Carhart M, Raasch C, Pierce J, Steffey D, Ostarello A (2006) Incidence of thoracic and lumbar spine injuries for restrained occupants in frontal collisions. Annu Proc Assoc Adv Automot Med 50:125–139
5. Smith JA, Siegel JH, Siddiqi SQ (2005) Spine and spinal cord injury in motor vehicle crashes: a function of change in velocity and energy dissipation on impact with respect to the direction of crash. J Trauma 59:117–131
6. Richter D, Hahn MP, Ostermann PA, Ekkernkamp A, Muhr G (1996) Vertical deceleration injuries: a comparative study of the injury patterns of 101 patients after accidental and intentional high falls. Injury 27:655–659
7. Inamasu J, Guiot BH (2007) Thoracolumbar junction injuries after motor vehicle collision: are there differences in restrained and nonrestrained front seat occupants? J Neurosurg Spine 7:311–314
8. Hsu JM, Joseph T, Ellis AM (2003) Thoracolumbar fracture in blunt trauma patients: guidelines for diagnosis and imaging. Injury 34:426–433
9. Aleman KB, Meyers MC (2010) Mountain biking injuries in children and adolescents. Sports Med 40: 77–90
10. Gertzbein SD, Khoury D, Bullington A, St John TA, Larson AI (2012) Thoracic and lumbar fractures associated with skiing and snowboarding injuries according to the AO Comprehensive Classification. Am J Sports Med 40:1750–1754
11. Alexander MJ (1985) Biomechanical aspects of lumbar spine injuries in athletes: a review. Can J Appl Sport Sci 10:1–20
12. Khan N, Husain S, Haak M (2008) Thoracolumbar injuries in the athlete. Sports Med Arthrosc Rev 16:16–25
13. Smiley JR (1964) Rcaf ejection experience: decade 1952–1961. Aerosp Med 35:125–129
14. Hearon B, Thomas H (1982) Mechanism of vertebral fracture in the F/FB-111 ejection experience. Aviat Space Environ Med 53:440–448
15. Edwards M (1996) Anthropometric measurements and ejection injuries. Aviat Space Environ Med 67: 1144–1147
16. Osborne RG, Cook AA (1997) Vertebral fracture after aircraft ejection during Operation Desert Storm. Aviat Space Environ Med 68:337–341
17. Williams CS (1993) F-16 pilot experience with combat ejections during the Persian Gulf War. Aviat Space Environ Med 64:845–847
18. Moreno Vazquez JM, Duran Tejeda MR, Garcia Alcon JL (1999) Report of ejections in the Spanish Air Force, 1979–1995: an epidemiological and comparative study. Aviat Space Environ Med 70: 686–691
19. Lewis ME (2006) Survivability and injuries from use of rocket-assisted ejection seats: analysis of 232 cases. Aviat Space Environ Med 77:936–943
20. Nakamura A (2007) Ejection experience 1956–2004 in Japan: an epidemiological study. Aviat Space Environ Med 78:54–58

21. Shanahan DF, Shanahan MO (1989) Injury in U.S. Army helicopter crashes October 1979-September 1985. J Trauma 29:415–422; discussion 423
22. Scullion JE, Heys SD, Page G (1987) Pattern of injuries in survivors of a helicopter crash. Injury 18: 13–14
23. Italiano P (1966) Vertebral fractures of pilots in helicopter accidents. Riv Med Aeronaut Spaz 29: 577–602
24. Helgeson MD, Lehman RA Jr, Cooper P, Frisch M, Andersen RC, Bellabarba C (2011) Retrospective review of lumbosacral dissociations in blast injuries. Spine 36:E469–E475
25. Ragel BT, Allred CD, Brevard S, Davis RT, Frank EH (2009) Fractures of the thoracolumbar spine sustained by soldiers in vehicles attacked by improvised explosive devices. Spine 34:2400–2405
26. Poopitaya S, Kanchanaroek K (2009) Injuries of the thoracolumbar spine from tertiary blast injury in Thai military personnel during conflict in southern Thailand. J Med Assoc Thai 92(Suppl 1):S129–S134
27. Schoenfeld AJ, Lehman RA Jr, Hsu JR (2012) Evaluation and management of combat-related spinal injuries: a review based on recent experiences. Spine J 12:817–823
28. Schoenfeld AJ, Goodman GP, Belmont PJ Jr (2012) Characterization of combat-related spinal injuries sustained by a US Army Brigade Combat Team during Operation Iraqi Freedom. Spine J 12:771–776
29. Blair JA, Patzkowski JC, Schoenfeld AJ, Cross Rivera JD, Grenier ES, Lehman RA Jr, Hsu JR (2012) Spinal column injuries among Americans in the global war on terrorism. J Bone Joint Surg Am 94:e135(131–139)
30. Lehman RA Jr, Paik H, Eckel TT, Helgeson MD, Cooper PB, Bellabarba C (2012) Low lumbar burst fractures: a unique fracture mechanism sustained in our current overseas conflicts. Spine J 12:784–790
31. Kang DG, Lehman RA Jr, Carragee EJ (2012) Wartime spine injuries: understanding the improvised explosive device and biophysics of blast trauma. Spine J 12:849–857
32. Holdsworth F (1970) Fractures, dislocations, and fracture-dislocations of the spine. J Bone Joint Surg Am 52:1534–1551
33. Ferguson RL, Allen BL Jr (1984) A mechanistic classification of thoracolumbar spine fractures. Clin Orthop Relat Res Oct:77–88
34. Larson SJ, Maiman DJ (1999) Surgery of the lumbar spine. Thieme, New York
35. Davies WE, Morris JH, Hill V (1980) An analysis of conservative (non-surgical) management of thoracolumbar fractures and fracture-dislocations with neural damage. J Bone Joint Surg Am 62:1324–1328
36. White AA, Panjabi MM (2013) Clinical biomechanics of the spine. Williams & Wilkins, Philadelphia
37. Westerborn A, Olsson O (1951) Mechanics, treatment and prognosis of fractures of the dorso-lumbar spine. Acta Chir Scand 102:59–83
38. Kaufer H, Hayes JT (1966) Lumbar fracture-dislocation. A study of twenty-one cases. J Bone Joint Surg Am 48:712–730
39. Chance GQ (1948) Note on a type of flexion fracture of the spine. Br J Radiol 21:452
40. Anderson PA, Rivara FP, Maier RV, Drake C (1991) The epidemiology of seatbelt-associated injuries. J Trauma 31:60–67
41. Howland WJ, Curry JL, Buffington CB (1965) Fulcrum fractures of the lumbar spine. Transverse fracture induced by an improperly placed seat belt. JAMA 193:240–241
42. Raney EM, Bennett JT (1992) Pediatric Chance fracture. Spine 17:1522–1524
43. Gallagher DJ, Heinrich SD (1990) Pediatric Chance fracture. J Orthop Trauma 4:183–187
44. Yoganandan N, Larson SJ, Pintar F, Maiman DJ, Reinartz J, Sances A Jr (1990) Biomechanics of lumbar pedicle screw/plate fixation in trauma. Neurosurgery 27:873–880; discussion 880–871
45. Shono Y, McAfee PC, Cunningham BW (1994) Experimental study of thoracolumbar burst fractures. A radiographic and biomechanical analysis of anterior and posterior instrumentation systems. Spine 19:1711–1722
46. Duma SM, Kemper AR, McNeely DM, Brolinson PG, Matsuoka F (2006) Biomechanical response of the lumbar spine in dynamic compression. Biomed Sci Instrum 42:476–481
47. Hongo M, Abe E, Shimada Y, Murai H, Ishikawa N, Sato K (1999) Surface strain distribution on thoracic and lumbar vertebrae under axial compression. The role in burst fractures. Spine 24:1197–1202
48. Langrana NA, Harten RR, Lin DC, Reiter MF, Lee CK (2002) Acute thoracolumbar burst fractures: a new view of loading mechanisms. Spine 27: 498–508
49. Shirado O, Zdeblick TA, McAfee PC, Cunningham BW, DeGroot H, Warden KE (1992) Quantitative histologic study of the influence of anterior spinal instrumentation and biodegradable polymer on lumbar interbody fusion after corpectomy. A canine model. Spine 17:795–803
50. Kazarian L, Graves GA (1977) Compressive strength characteristics of the human vertebral centrum. Spine 2:1–14
51. Ochia RS, Tencer AF, Ching RP (2003) Effect of loading rate on endplate and vertebral body strength in human lumbar vertebrae. J Biomech 36: 1875–1881
52. Perey O (1957) Fracture of the vertebral end-plate in the lumbar spine; an experimental biochemical investigation. Acta Orthop Scand Supplementum 25:1–101
53. Alkalay RN, von Stechow D, Torres K, Hassan S, Sommerich R, Zurakowski D (2008) The effect of cement augmentation on the geometry and structural response of recovered osteopenic vertebrae: an anterior-wedge fracture model. Spine 33:1627–1636

54. Belkoff SM, Mathis JM, Jasper LE, Deramond H (2001) The biomechanics of vertebroplasty. The effect of cement volume on mechanical behavior. Spine 26:1537–1541
55. Hansson T, Roos B, Nachemson A (1980) The bone mineral content and ultimate compressive strength of lumbar vertebrae. Spine 5:46–55
56. Steens J, Verdonschot N, Aalsma AM, Hosman AJ (2007) The influence of endplate-to-endplate cement augmentation on vertebral strength and stiffness in vertebroplasty. Spine 32:E419–E422
57. Bartley MH Jr, Arnold JS, Haslam RK, Jee WS (1966) The relationship of bone strength and bone quantity in health, disease, and aging. J Gerontol 21:517–521
58. Bell GH, Dunbar O, Beck JS, Gibb A (1967) Variations in strength of vertebrae with age and their relation to osteoporosis. Calcif Tissue Res 1:75–86
59. Skaggs DL, Weidenbaum M, Iatridis JC, Ratcliffe A, Mow VC (1994) Regional variation in tensile properties and biochemical composition of the human lumbar anulus fibrosus. Spine 19:1310–1319
60. Ebara S, Iatridis JC, Setton LA, Foster RJ, Mow VC, Weidenbaum M (1996) Tensile properties of nondegenerate human lumbar anulus fibrosus. Spine 21: 452–461
61. Acaroglu ER, Iatridis JC, Setton LA, Foster RJ, Mow VC, Weidenbaum M (1995) Degeneration and aging affect the tensile behavior of human lumbar anulus fibrosus. Spine 20:2690–2701
62. Green TP, Adams MA, Dolan P (1993) Tensile properties of the annulus fibrosus II. Ultimate tensile strength and fatigue life. Eur Spine J 2:209–214
63. Ambrosetti-Giudici S, Gedet P, Ferguson SJ, Chegini S, Burger J (2010) Viscoelastic properties of the ovine posterior spinal ligaments are strain dependent. Clin Biomech 25:97–102
64. Lucas SR, Bass CR, Crandall JR, Kent RW, Shen FH, Salzar RS (2009) Viscoelastic and failure properties of spine ligament collagen fascicles. Biomech Model Mechanobiol 8:487–498
65. Bass CR, Planchak CJ, Salzar RS, Lucas SR, Rafaels KA, Shender BS, Paskoff G (2007) The temperature-dependent viscoelasticity of porcine lumbar spine ligaments. Spine 32:E436–E442
66. Lu WW, Luk KD, Holmes AD, Cheung KM, Leong JC (2005) Pure shear properties of lumbar spinal joints and the effect of tissue sectioning on load sharing. Spine 30:E204–E209
67. Iida T, Abumi K, Kotani Y, Kaneda K (2002) Effects of aging and spinal degeneration on mechanical properties of lumbar supraspinous and interspinous ligaments. Spine J 2:95–100
68. Neumann P, Keller TS, Ekstrom L, Hansson T (1994) Effect of strain rate and bone mineral on the structural properties of the human anterior longitudinal ligament. Spine 19:205–211
69. Neumann P, Ekstrom LA, Keller TS, Perry L, Hansson TH (1994) Aging, vertebral density, and disc degeneration alter the tensile stress-strain characteristics of the human anterior longitudinal ligament. J Orthop Res 12:103–112
70. Pintar FA, Yoganandan N, Myers T, Elhagediab A, Sances A Jr (1992) Biomechanical properties of human lumbar spine ligaments. J Biomech 25: 1351–1356
71. Neumann P, Keller TS, Ekstrom L, Perry L, Hansson TH, Spengler DM (1992) Mechanical properties of the human lumbar anterior longitudinal ligament. J Biomech 25:1185–1194
72. Hukins DW, Kirby MC, Sikoryn TA, Aspden RM, Cox AJ (1990) Comparison of structure, mechanical properties, and functions of lumbar spinal ligaments. Spine 15:787–795
73. Hasberry S, Pearcy MJ (1986) Temperature dependence of the tensile properties of interspinous ligaments of sheep. J Biomed Eng 8:62–66
74. Nachemson AL, Evans JH (1968) Some mechanical properties of the third human lumbar interlaminar ligament (ligamentum flavum). J Biomech 1:211–220
75. Tkaczuk H (1968) Tensile properties of human lumbar longitudinal ligaments. Acta Orthop Scand Suppl 115:111+
76. Zhu D, Gu G, Wu W, Gong H, Zhu W, Jiang T, Cao Z (2008) Micro-structure and mechanical properties of annulus fibrous of the L4-5 and L5-S1 intervertebral discs. Clin Biomech 23(Suppl 1):S74–S82
77. Hirsch C (1955) The reaction of intervertebral discs to compression forces. J Bone joint Surg Am 37-A: 1188–1196
78. Willen J, Lindahl S, Irstam L, Aldman B, Nordwall A (1984) The thoracolumbar crush fracture. An experimental study on instant axial dynamic loading: the resulting fracture type and its stability. Spine 9:624–631
79. Oxland TR, Panjabi MM, Lin RM (1994) Axes of motion of thoracolumbar burst fractures. J Spinal Disord 7:130–138
80. Fredrickson BE, Mann KA, Yuan HA, Lubicky JP (1988) Reduction of the intracanal fragment in experimental burst fractures. Spine 13:267–271
81. Mermelstein LE, McLain RF, Yerby SA (1998) Reinforcement of thoracolumbar burst fractures with calcium phosphate cement. A biomechanical study. Spine 23:664–670; discussion 670–661
82. Kallemeier PM, Beaubien BP, Buttermann GR, Polga DJ, Wood KB (2008) In vitro analysis of anterior and posterior fixation in an experimental unstable burst fracture model. J Spinal Disord Tech 21:216–224
83. Jones HL, Crawley AL, Noble PC, Schoenfeld AJ, Weiner BK (2011) A novel method for the reproducible production of thoracolumbar burst fractures in human cadaveric specimens. Spine J 11:447–451
84. Kifune M, Panjabi MM, Liu W, Arand M, Vasavada A, Oxland T (1997) Functional morphology of the spinal canal after endplate, wedge, and burst fractures. J Spinal Disord 10:457–466

85. Panjabi MM, Kifune M, Wen L, Arand M, Oxland TR, Lin RM, Yoon WS, Vasavada A (1995) Dynamic canal encroachment during thoracolumbar burst fractures. J Spinal Disord 8:39–48
86. Stemper BD, Storvik SG, Yoganandan N, Baisden JL, Fijalkowski RJ, Pintar FA, Shender BS, Paskoff GR (2011) A new PMHS model for lumbar spine injuries during vertical acceleration. J Biomech Eng 133:081002
87. Gozulov SA, Korzhen'iants VA, Skrypnik VG, Sushkov Iu N (1966) Study of the durability of the human vertebrae under compression. Arkh Anat Gistol Embriol 51:13–18
88. Ash JH, Kerrigan JR, Arregui-Dalmases C, Del Pozo E, Crandall J (2010) Endplate indentation of the fourth lumbar vertebra – biomed 2010. Biomed Sci Instrum 46:160–165
89. Labrom RD, Tan JS, Reilly CW, Tredwell SJ, Fisher CG, Oxland TR (2005) The effect of interbody cage positioning on lumbosacral vertebral endplate failure in compression. Spine 30:E556–E561
90. Hansson T, Roos B (1980) The influence of age, height, and weight on the bone mineral content of lumbar vertebrae. Spine 5:545–551
91. Hou Y, Yuan W (2012) Influences of disc degeneration and bone mineral density on the structural properties of lumbar end plates. Spine J 12:249–256
92. Closkey RF, Parsons JR, Lee CK, Blacksin MF, Zimmerman MC (1993) Mechanics of interbody spinal fusion. Analysis of critical bone graft area. Spine 18:1011–1015
93. Hollowell JP, Vollmer DG, Wilson CR, Pintar FA, Yoganandan N (1996) Biomechanical analysis of thoracolumbar interbody constructs. How important is the endplate? Spine 21:1032–1036
94. Jost B, Cripton PA, Lund T, Oxland TR, Lippuner K, Jaeger P, Nolte LP (1998) Compressive strength of interbody cages in the lumbar spine: the effect of cage shape, posterior instrumentation and bone density. Eur Spine J 7:132–141
95. Stemper BD, Yoganandan N, Baisden JL, Pintar FA, Shender BS (2012) Rate-dependent failure characteristics of thoraco-lumbar vertebrae: application to the military environment. In: Proceedings of the ASME 2012 summer bioengineering conference, Fajardo
96. Hirsch C, Nachemson A (1954) New observations on the mechanical behavior of lumbar discs. Acta Orthop Scand 23:254–283
97. Denis F (1983) The three column spine and its significance in the classification of acute thoracolumbar spinal injuries. Spine 8:817–831
98. Dai LY, Yao WF, Cui YM, Zhou Q (2004) Thoracolumbar fractures in patients with multiple injuries: diagnosis and treatment-a review of 147 cases. J Trauma 56:348–355
99. Wittenberg RH, Hargus S, Steffen R, Muhr G, Botel U (2002) Noncontiguous unstable spine fractures. Spine 27:254–257
100. Kifune M, Panjabi MM, Arand M, Liu W (1995) Fracture pattern and instability of thoracolumbar injuries. Eur Spine J 4:98–103
101. Panjabi MM, Kifune M, Liu W, Arand M, Vasavada A, Oxland TR (1998) Graded thoracolumbar spinal injuries: development of multidirectional instability. Eur Spine J 7:332–339
102. Panjabi MM, Oxland TR, Kifune M, Arand M, Wen L, Chen A (1995) Validity of the three-column theory of thoracolumbar fractures. A biomechanic investigation. Spine 20:1122–1127
103. Ochia RS, Ching RP (2002) Internal pressure measurements during burst fracture formation in human lumbar vertebrae. Spine 27:1160–1167
104. Ewing CL (1966) Vertebral fracture in jet aircraft accidents: a statistical analysis for the period 1959 through 1963, U. S. Navy. Aerosp Med 37:505–508
105. Harrison WD (1979) Ejection experience in F/FB-111 Aircraft/1967–1978. Safe J
106. Smelsey SO (1970) Study of pilots who have made multiple ejections. Aerosp Med 41:563–566
107. Smiley JR (1965) RCAF ejection experience 1952–1961. RCAF Institute of Aviation Medicine, Toronto, pp 18
108. Sandstedt P (1989) Experiences of rocket seat ejections in the Swedish Air Force: 1967–1987. Aviat Space Environ Med 60:367–373
109. Eiband AM (1959) Human tolerance to rapidly applied accelerations: a summary of the literature. National Aeronautics and Space Administration (NASA), Washington, DC
110. Weiss MS, Matson DL, Mawn SV (1989) Guidelines for safe human exposure to impact acceleration. Naval Biodynamics Laboratory, New Orleans
111. Latham F (1957) A study in body ballistics: seat ejection. Proc R Soc Lond B Biol Sci 147:121–139
112. Stech EI, Payne PR (1969) Dynamic models of the human body. Aerospace Medical Research Laboratory
113. Brown T, Hansen RJ, Yorra AJ (1957) Some mechanical tests on the lumbosacral spine with particular reference to the intervertebral discs; a preliminary report. J Bone Joint Surg Am 39-A:1135–1164
114. Coermann RR (1962) The mechanical impedance of the human body in sitting and standing position at low frequencies. Hum Factors 4:227–253
115. Brinkley JW, Shaffer JT (1971) Dynamic simulation techniques for the design of escape systems: current applications and future air force requirements. Wright-Patterson Air Force Base
116. Chandler R (1985) Human injury criteria relative to civil aircraft seat and restraint systems. Society of Automotive Engineers (SAE), 851847